

## Facile Synthesis of Processible Aminoquinoline/Phenetidine Copolymers and Their Pure Semiconducting Nanoparticles

Xin-Gui Li, Mei-Rong Huang, and Yi-Min Hua

*Macromolecules*, 2005, 38 (10), 4211-4219 • DOI: 10.1021/ma047581n • Publication Date (Web): 16 April 2005

Downloaded from <http://pubs.acs.org> on February 13, 2009

### More About This Article

Additional resources and features associated with this article are available within the HTML version:

- Supporting Information
- Links to the 3 articles that cite this article, as of the time of this article download
- Access to high resolution figures
- Links to articles and content related to this article
- Copyright permission to reproduce figures and/or text from this article

[View the Full Text HTML](#)



# Facile Synthesis of Processible Aminoquinoline/Phenetidine Copolymers and Their Pure Semiconducting Nanoparticles

Xin-Gui Li,<sup>\*,†,‡</sup> Mei-Rong Huang,<sup>‡</sup> and Yi-Min Hua<sup>§</sup>

Department of Chemistry & Chemical Biology, Harvard University, 12 Oxford Street, Cambridge, Massachusetts 02138; Institute of Materials Chemistry, School of Materials Science & Engineering, Tongji University, 1239 Siping Road, Shanghai 200092, China; and Department of Chemistry, The University of Arizona, Tucson, Arizona 85721

Received November 22, 2004; Revised Manuscript Received January 12, 2005

**ABSTRACT:** A series of fine copolymer particles from 8-aminoquinoline (AQ) and *o*-phenetidine (PD) were simply synthesized by a chemical oxidative polymerization in three aqueous media. The potential and temperature of polymerization solution were effectively employed to pursue the polymerization progress. The molecular and morphological structures of the resulted AQ/PD copolymer particles were thoroughly characterized by IR, UV-vis, NMR, gel permeation chromatography, laser particle size analysis, and atomic force microscopy. An important dependency of polymerization yield, structure, and properties of the particles on AQ/PD ratio, temperature, and medium of polymerization has been found. The size of the AQ/PD copolymer base particles exhibits a monotonic decrease with increasing AQ content from 5 to 100 mol %. A facile technique of preparing semiconducting pure nanoparticles by introducing the AQ units with positively charged quaternary ammonium groups but without adsorptive stabilizer or sulfonic groups is created for the first time. Both the molecular weight and bulk electrical conductivity of the copolymers display an utmost at AQ content of 5 mol %, while polymerization yield and bulk electrical conductivity seem to be the highest at the lowest polymerization temperature of 5 °C. The solubility and film formability of the copolymers are superior in highly polar solvents and achieve the best at an AQ content of 5–10 mol %.

## 1. Introduction

Polyaniline (PAN) and its derivatives are novel conducting polymers that have been extensively studied for electronic, optical, chemical, and biological applications because they have a simple and reversible acid/base doping/dedoping chemistry enabling control over properties<sup>1–3</sup> such as free volume, solubility, electroconductivity, electrochromism, electrocatalysis, electroactivity, optical activity, ion absorbability,<sup>2,3</sup> and gas permselectivity. Nanoscale conducting polymer including nanoparticles, nanowires, nanofilms, and nanocomposites has been investigated with the expectation that such polymer will possess the advantages of both organic semiconductors and nanomaterials.<sup>1,4,5</sup> Recently, a new oxidative polymer from nitrogen heterocyclic aromatic amine has been facilely synthesized by electropolymerization. The polymer contains a  $-C=N-C-$  group in the aromatic ring as one more redox site than PAN. Therefore, the heterocyclic polymer is anticipated as a multifunctional material that presents further better properties than conventional nonheterocyclic polymer. Therefore, the heterocyclic polymer could be served as a new advanced material with potential applicability.

The oxidative polymer from aminoquinoline as a typical bifunctional nitrogen heterocyclic aromatic amine shows some unique properties similar to other polymers from nitrogen heterocyclic aromatic amine.<sup>6,7</sup> It is reported that the quinoline and its derivatives can electropolymerize into compact polymer films with an even surface as well as good mechanical properties.<sup>6,8</sup> However, the film area and shape depend completely

on the characteristics of the electrode used. In addition, the poor solubility of the heterocyclic polymers limits their widely realistic appliance. Fortunately, it has been found that PAN derivatives exhibit a remarkably enhanced solubility and therefore a significantly improved processibility as compared with PAN.<sup>1,9</sup> As an aniline derivative, *o*-phenetidine (PD) is frequently utilized to copolymerize with other aromatic monomers for a significant improvement of the polymer solubility and furthermore the processibility.<sup>10</sup> Chemically oxidative copolymerization of aminoquinoline and PD might resolve these problems, but no study focuses on it at all until now.

In this article, a successful chemical oxidative copolymerization of 8-aminoquinoline (AQ) with PD is carried out as one of the best methods to combine the advantages of the two homopolymers. The polymerization characteristics, structure, and properties of the AQ/PD copolymer fine particles were systematically elaborated. A new facile technique to prepare the pure polymer particles with the diameter of down to ~14 nm by a simple chemical oxidative polymerization in aqueous media without external additives or internal ionic side groups as stabilizer was proposed for the first time.

## 2. Experimental Section

**2.1. General.** 8-Aminoquinoline (AQ), *o*-phenetidine (PD), ammonium persulfate, HCl, H<sub>2</sub>SO<sub>4</sub>, acetonitrile (MeCN), dimethyl sulfoxide (DMSO), *N*-methylpyrrolidone (NMP), chloroform (CHCl<sub>3</sub>), and tetrahydrofuran (THF) were commercially obtained as chemical pure reagents and used without further purification.

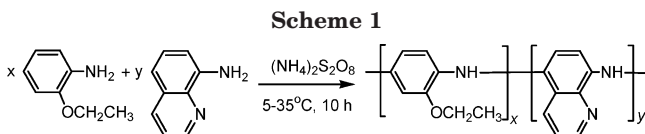
The AQ/PD copolymerization was followed by the open-circuit potential (OCP) profile technique, using a saturated calomel electrode (SCE) as reference electrode and a Pt electrode as a working electrode. The bulk electrical conductivity of the salt and base of AQ/PD copolymers was measured by the following method: put about 10 mg copolymer powders between two round-disk stainless iron electrodes with a

<sup>†</sup> Harvard University.

<sup>‡</sup> Tongji University.

<sup>§</sup> The University of Arizona.

\* To whom correspondence should be addressed: e-mail [lixingui@tongji.edu.cn](mailto:lixingui@tongji.edu.cn); Ph +86-21-65980524; Fax 86-21-65980530. The present address is Tongji University.



diameter of 1 cm and press the powder tight to a pellet and then measure the resistance and thickness of the copolymer pellet with a multimeter and a thickness gauge, respectively. The redoped salt samples were prepared by doping AQ/PD copolymers with 1 M HCl aqueous solution for 48 h. The copolymer solubility was evaluated as follows: polymer powder of about 2 mg was added to 1 mL of solvent and dispersed thoroughly after shaking intermittently for 2 h at ambient temperature. The film formability was studied with NMP as solvent at the concentration of 30 mg of copolymer in 3 mL of solvent by a solution-casting method. The NMP in copolymer solution on glass with the area of  $3 \times 3 \text{ cm}^2$  was evaporated at around  $70^\circ\text{C}$ .

IR spectra were recorded on a Nicolet Magna-IR 550 spectrometer at  $2 \text{ cm}^{-1}$  resolution on KBr pellets. High-resolution  $^1\text{H}$  NMR spectra were obtained in deuterated  $\text{DMSO-}d_6$  using Bruker DMX 500 spectrometer operating at 500.13 MHz after the scanning number of 64. UV-vis spectra of a homogeneous solution of AQ/PD copolymer bases at a concentration of 0.0125 mg/mL in NMP were recorded on Perkin-Elmer Instruments Lambda 35 in a range of 110–190 nm at a scanning rate of 480 nm/min. Molecular weight of the AQ/PD copolymers was measured using an HP1100 GPC column (PL-gel mixed C  $\times$  2, PL gel 50 nm) and THF as solvent and mobile phase as well as monodisperse polystyrene (MW 500– $10^6$  g/mol) as standard. The size and its distribution of the copolymer fine particles formed just after polymerization or dedoping treatment were analyzed on a Beckman Coulter LS230 laser particle size analyzer (LPSA). The fine copolymer particles were observed by an SPA-300HV AFM system, Seiko SII Instruments, Japan.

**2.2. Preparation of the Fine Particles of the Copolymers.** AQ/PD copolymer particles were simply prepared by a chemical oxidative polymerization of AQ with PD monomers. A typical procedure for the preparation of AQ/PD (10/90) copolymer is as follows: to 10 mL of 1 M HCl aqueous solution in a 50 mL glass flask in a water bath at  $5^\circ\text{C}$  was added 0.147 g of AQ (1 mmol) and 1.29 mL of PD (9 mmol) and then stirred vigorously for half an hour. An oxidant solution was prepared separately by dissolving 2.327 g (10 mmol) of ammonium persulfate  $[(\text{NH}_4)_2\text{S}_2\text{O}_8]$  in 5 mL of 1 M HCl aqueous solution. The monomer solution was then treated with the oxidant solution by dropwise adding the oxidant solution at a rate of one drop per 3 s. The reaction mixture was stirred continuously for 10 h at  $5^\circ\text{C}$  together with the measurement of the OCP and temperature of the polymerization solution. After that, the copolymer HCl salt particles as precipitates were isolated from the reaction mixture by filtration and washed with an excess of distilled water in order to remove the remaining oxidant and water-soluble oligomer. The HCl salt was subsequently neutralized in 0.2 M ammonium hydroxide of 100 mL, stirring overnight. The final polymer particles were left to dry in ambient air for 1 week, obtaining the emeraldine base of AQ/PD (10/90) copolymer as black solid powders. The nominal polymerization is shown in Scheme 1.

When using MeCN as polymerization medium, AQ/PD monomers were added to 10 mL of MeCN. An oxidant solution was prepared separately by dissolving ammonium persulfate  $[(\text{NH}_4)_2\text{S}_2\text{O}_8]$  in 5 mL of distilled water. The other procedure is almost the same as above.

### 3. Results and Discussion

#### 3.1. Copolymerization of AQ and PD Monomers.

The chemical oxidative copolymerization between AQ and PD monomers of various ratios affords a dark precipitate as products. The color of the products changed from black to brown with increasing AQ

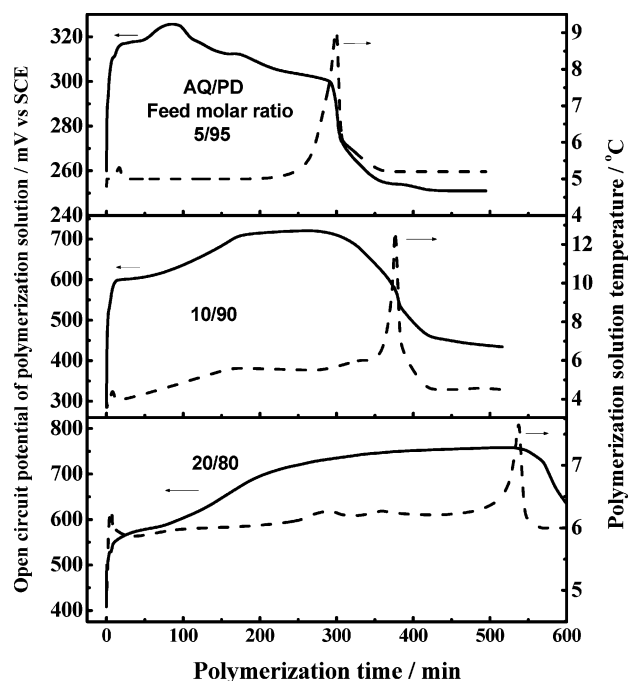


**Figure 1.** Solution OCP- and temperature-time curves of chemical oxidative polymerization of 8-aminoquinoline (AQ) and *o*-phenetidine (PD) with AQ/PD feed molar ratios of 5/95, 10/90, and 20/80 in 1 M HCl aqueous solution at the initial solution temperature of  $4\text{--}5^\circ\text{C}$ .

content from 0 to 100 mol %. The AQ/PD copolymerization process was in-situ followed by measurement of the OCP and temperature of the reaction solution, which may provide a deeper insight into polymerization process, as shown in Figure 1. The initial OCP of PD monomer in 1 M HCl was 250 mV vs SCE, which was an equilibrium potential for the protonated PD monomer after a time lapse of 0.5 h. After adding AQ monomer to the PD solution, the initial OCP of the comonomer solution increased to 260–400 mV vs SCE. When the oxidant solution was added to the AQ/PD comonomer solution, an immediate and fast OCP increase was detected. Apparently, the variation of solution OCP displays three stages: increasing, relatively steady, and decreasing. A similar situation was observed during the chemical oxidative polymerization of aniline.<sup>11</sup> The OCP increased continuously in the first stage ( $t_1$ ) owing to dissociation of the persulfate ions to radical anions,  $\text{SO}_4^{\cdot-}$ , and anion,  $\text{SO}_4^{2-}$ , in the presence of monomers. In this stage, the formed oligomers can act as a reductant. The oxidized oligomers could propagate subsequent polymerization with residual monomers via an electrophilic aromatic substitution mechanism. Accompanying the OCP change, the color of the polymerization solution deepened constantly.

As the copolymerization proceeded, the OCP reached a steady plateau ranging from 320 to 750 mV vs SCE. In the second stage, the AQ/PD copolymer chains formed in the first stage might be further oxidized by the residual oxidant. The propagation may proceed on the oxidized chains to afford a higher molecular weight copolymer. These newly formed AQ/PD copolymer chains may also be oxidized to participate in the chain propagation. This process is repeated until all the oxidant is used up at the end of the plateau stage ( $t_2$ ). Following the plateau stage, the OCP decreased steadily. This third stage ( $t_3$ ) may involve further copolymerization of monomers with the oxidized copolymer chain that

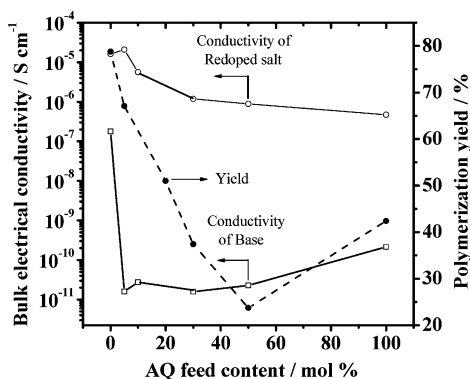


**Figure 2.** Polymerization yield and bulk electrical conductivity (recorded at 18 °C) of 8-aminoquinoline (AQ)/*o*-phenetidine (PD) copolymers with different AQ feed content prepared in 1 M HCl aqueous solution at 5 °C.

formed in the second stage as the oxidant instead of ammonium persulfate. According to Wei's conclusion,<sup>12</sup> the time elapsed at the end of the plateau, i.e.,  $t_1 + t_2$ , reflects the copolymerization rate. As seen in Figure 1,  $t_1 + t_2$  increased with enhancing AQ content, implying that the copolymerization rate slowed down with increasing AQ content. A possible reason is that the steric hindrance of the AQ ring is larger than that of PD ring, resulting in more difficult electrophilic reaction between monomers and propagating chains.

It is found from Figure 2 that the AQ/PD polymerization yield significantly depends on the monomer ratio. The yield decreases from the highest value (80%) to the lowest value (25%) as AQ feed content increases from 0 to 50 mol %. With a further increase of AQ feed content to 100 mol %, the yield increases to a medium value (42.5%). This indicates a lower copolymerizability between AQ and PD comonomers than individual PD or AQ homopolymerizability. In other words, the chain propagations between activated PD end group and AQ monomer (or between activated AQ end group and PD monomer) are passivated by each other, i.e., a retardation between PD (or AQ) end group and AQ (or PD) monomer. This retardant copolymerization finally results in lower yield of copolymerization than that of respective homopolymerizations. This should be an indication of a strong interaction between AQ and PD monomers; i.e., a real copolymerization occurred between them.

It is seen from Figure 1 that the solution temperature during AQ/PD copolymerization in HCl increases with polymerization time and reaches a maximum at a certain time. The maximum temperature and corresponding polymerization time depend on AQ/PD ratio. At the AQ/PD molar ratio of 10/90, the maximum temperature reaches up to the highest (13 °C), suggesting the strongest exothermic copolymerization. It is observed from Figure 3 that the maximal solution temperature and corresponding polymerization time during AQ/PD (10/90) copolymerization in HCl vary remarkably with initial polymerization temperature. The maximum temperature depends on the initial solution temperature. At the initial temperature of 25 and 35 °C, the maximum temperature reaches up to 27.5 and 41.5 °C at 68 and 30 min, respectively, suggesting an exothermic copolymerization. Furthermore, the higher the initial reaction temperature, the greater the reaction exotherm is. This phenomenon may be due to the higher oxidative rate of the oxidant at

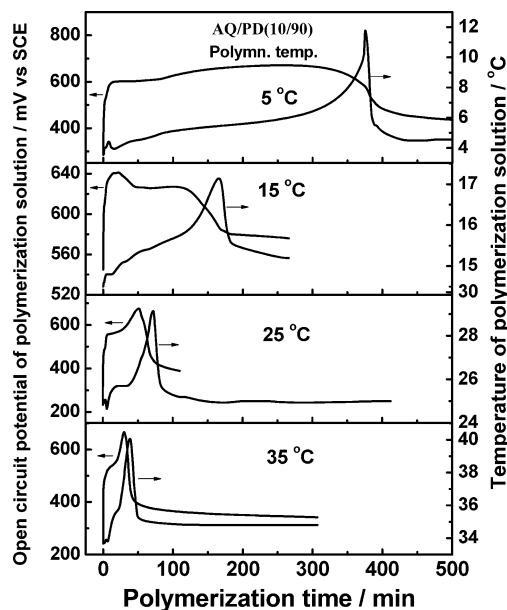


**Figure 3.** Solution OCP and temperature during chemical oxidative copolymerization of 8-aminoquinoline (AQ) and *o*-phenetidine (PD) with AQ/PD feed molar ratio of 10/90 in 1 M HCl aqueous solution at 5–35 °C, respectively.

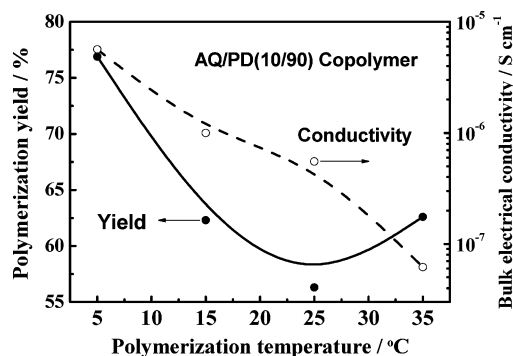


**Figure 4.** Influence of polymerization temperature on polymerization yield of 8-aminoquinoline (AQ)/*o*-phenetidine (PD) (10/90) copolymer bases prepared in 1 M HCl aqueous solution and on their conductivity (recorded at 10 °C) after redoped in 1 M HCl aqueous solution.

higher temperature, resulting in faster creation of active centers in the system and then more dramatic polymerization. Therefore, a significant dependence of the copolymerization yield on the polymerization temperature is shown in Figure 4. The AQ/PD (10/90) copolymerization yield reached the highest value of 77.3% at the initial reaction temperature of 5 °C, together with the highest electrical conductivity, indicating that the optimal copolymerization temperature could be 5 °C. It can be concluded that low solution temperature favors the copolymerization because the chain termination rate could be relatively slow at the low temperature.

Synthesis of conducting polymer is based on a generally accepted radical cation mechanism in acidic medium. In this paper, AQ/PD copolymer was also successfully prepared in the mixture of MeCN and water without adding any acid. An influence of polymerization medium on the AQ/PD (10/90) copolymerization is shown in Figure 5 and Table 1. The AQ/PD (10/90) reaction temperature in the MeCN/water mixture reached a maximal value much earlier than those in other two acidic media, suggesting that the oxidation rate of AQ and PD monomers to form copolymer

**Table 1. Influence of Polymerization Media on the Polymerization Yield, Size, and Conductivity of 8-Aminoquinoline (AQ)/*o*-Phenetidine (PD) (10/90) Copolymer Particles Prepared at 25 °C**

	polymerization medium	1 M HCl	0.5 M H <sub>2</sub> SO <sub>4</sub>	MeCN + H <sub>2</sub> O <sup>a</sup>
polymerization yield (%)		56.3	59.2	49.4
particle diameter in water (μm)	virgin salt	7.603	7.119	
	base	2.307	0.441	2.266
standard deviation of the particle diameter in water (μm)	virgin salt	4.480	3.442	
	base	2.473	0.556	1.379
conductivity of copolymers redoped in 1 M HCl (S cm <sup>-1</sup> ) <sup>b</sup>		5.54 × 10 <sup>-7</sup>	7.9 × 10 <sup>-7</sup>	2.34 × 10 <sup>-7</sup>

<sup>a</sup> Volume ratio of MeCN to H<sub>2</sub>O = 2:1. <sup>b</sup> Recorded at 10 °C.

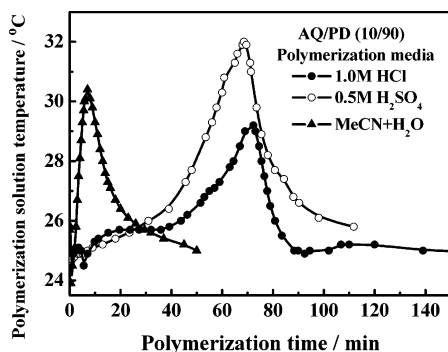


**Figure 5.** Temperature of 8-aminoquinoline (AQ)/*o*-phenetidine (PD) (10/90) copolymerization solution during the polymerization process at 25 °C in 1 M HCl aqueous solution, 0.5 M H<sub>2</sub>SO<sub>4</sub> aqueous solution, and a mixture of MeCN and H<sub>2</sub>O with a volume ratio of 2/1, respectively.

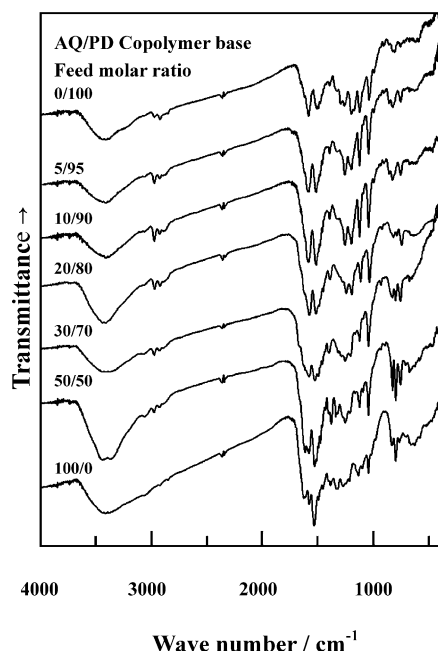


**Figure 6.** IR spectra of 8-aminoquinoline (AQ)/*o*-phenetidine (PD) copolymer bases prepared in 1 M HCl aqueous solution at 5 °C with AQ/PD feed molar ratios of 0/100, 5/95, 10/90, 20/80, 30/70, 50/50, and 100/0.

becomes higher on increasing the pH value of the medium due to its deprotonation effect. Such behavior was also reported in aniline polymerization in ref 11 as well as pyrrole/phenetidine copolymerization.<sup>13</sup> Note that the polymerization yield in MeCN/water seems to be the lowest.

**3.2. IR Spectra of the Copolymers.** The IR spectra for the seven AQ/PD copolymers are shown in Figure 6. Apparently, a systematical spectral variation with AQ/PD ratio has been observed. A broad absorption band at 3408–3441 cm<sup>-1</sup> due to characteristic N–H

stretching vibration suggests the presence of secondary amino groups. The peak at 3065 cm<sup>-1</sup> should be assigned to aromatic C–H stretching vibration. Three weak peaks at 2978/2926 and 2869 cm<sup>-1</sup> correspond to aliphatic C–H asymmetric and symmetric stretching vibration of the PD ethyl groups, respectively.<sup>14</sup> With increasing AQ content, all the three peaks mentioned above become weaker because the AQ unit does not contain any aliphatic C–H bond. Absorption peaks appearing at 1573 and 1505 cm<sup>-1</sup> are attributed respectively to the quinoid and benzenoid rings in the copolymer, caused by stretching vibration of C=N bonds in the diiminoquinoid ring and skeletal vibration of the benzenoid aromatic ring, respectively.<sup>15</sup> It is seen that the absorption peak due to the quinoid ring shifts to higher wavenumber, and its relative intensity increases slightly as AQ content increases, but the peak intensity at 1505 cm<sup>-1</sup> increases significantly. When AQ feed content ranges between 50 and 100 mol %, a new absorption peak appears around 1565 cm<sup>-1</sup> that should correspond to in-plane bending vibration of N–H in secondary amine group in AQ units. This peak might overlap by the stretching vibration peak of C=N bonds in the diiminoquinoid ring when AQ content is low.<sup>16</sup> The medium absorption peak centered at 1247 cm<sup>-1</sup> should be ascribed to the C–N stretching vibration. It also confirms that PD units in the copolymer exist as more quinoid structure. The peak at 1118 cm<sup>-1</sup> owing to the C–H in-plane bending vibration of the 1,2,4-trisubstituted benzene ring gets stronger with increasing PD content, indicating that the peak is attributed to PD units. The presence of the trisubstituted PD units and secondary amino groups suggests the formation of polymers. By the way, the small peaks at around 2350 cm<sup>-1</sup> would be attributed to the surrounding carbon dioxide.

The IR spectra of AQ/PD (10/90) copolymers prepared at different polymerization temperatures or in various media are similar to each other, indicating similar copolymer structure. Therefore, the polymerization temperature and medium have little impact on the molecular structure of the AQ/PD copolymer. However, the absorption peak due to quinoid ring becomes stronger with elevating polymerization temperature, implying higher quinoid content due to higher oxidative ability.

**3.3. UV–Vis Spectra of the Copolymers.** UV–vis spectra of the AQ/PD copolymer bases with different AQ/PD ratios are compared in detail in Figure 7. A strong band and a broad but relatively weak band can be observed in these UV–vis spectra. When AQ feed content is less than 10 mol %, the strong absorption band at 273–277 nm (band I) is assigned to the  $\pi$ – $\pi^*$  transition of the benzenoid ring, and the relatively weak band around 612–614 nm (band II) is attributed to excitation transition from the benzenoid ring to quinoid ring.<sup>17</sup> Both of the transitions are related to the extension of the conjugation along the molecular chain. It is

**Table 2. Intensity Ratio of Exciton Transition Band (Band II)/ $\pi$ - $\pi^*$  Transition Band (Band I) from UV-Vis Spectra (in NMP) of 8-Aminoquinoline (AQ)/*o*-Phenetidine (PD) Copolymer Bases with Different AQ/PD Ratios, Prepared at Various Polymerization Temperatures or Media**

AQ/PD feed molar ratio	polymerization		band I		band II		intensity ratio of band II/I
	temperature (°C)	medium	wavelength (nm)	intensity	wavelength (nm)	intensity	
0/100	5	1 M HCl	277	1.021	618	0.237	0.23
5/95	5	1 M HCl	274	0.952	608	0.118	0.12
10/90	5	1 M HCl	273	1.311	607	0.255	0.19
20/80	5	1 M HCl	273	1.312	467	0.304	0.23
30/70	5	1 M HCl	280	0.779	468	0.349	0.45
50/50	5	1 M HCl	273	0.950	476	0.248	0.26
100/0	5	1 M HCl	267	1.143	478	0.203	0.18
10/90	15	1 M HCl	278	0.840	586	0.216	0.26
10/90	25	1 M HCl	276	0.711	504	0.212	0.30
10/90	35	1 M HCl	278	0.997	486	0.323	0.32
10/90	25	0.5 M H <sub>2</sub> SO <sub>4</sub>	291	0.641	489	0.236	0.37
10/90	25	MeCN + H <sub>2</sub> O	279	0.552	452	0.215	0.39

seen from Table 2 that band II dramatically shows a blue shift to 467–478 nm when the AQ feed content is more than 20 mol %, indicating a diminution in the extension of the conjugation system along the molecular chain, probably due to a decrease in the molecular weight and/or lower content of quinoid structure in the more AQ unit-containing copolymer. This behavior is accordant with the IR spectral results. It can also be observed from Figure 8 and Table 2 that band II of AQ/PD(10/90) copolymers obtained at an elevated temperature or in a neutral medium shows a significant shift to short wavelength, suggesting shorter conjugating length, i.e., lower molecular weight. However, the AQ/PD(10/90) copolymer formed at 35 °C or in MeCN + H<sub>2</sub>O

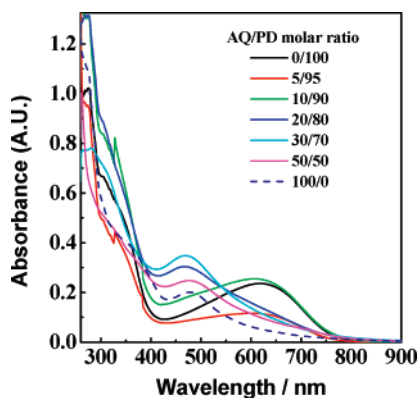


**Figure 7.** UV-vis spectra of the NMP solution at a concentration of 0.0125 mg/mL of AQ/PD copolymer bases prepared at 5 °C in 1 M HCl aqueous solution with AQ/PD feed molar ratios of 0/100, 5/95, 10/90, 20/80, 30/70, 50/50, and 100/0.

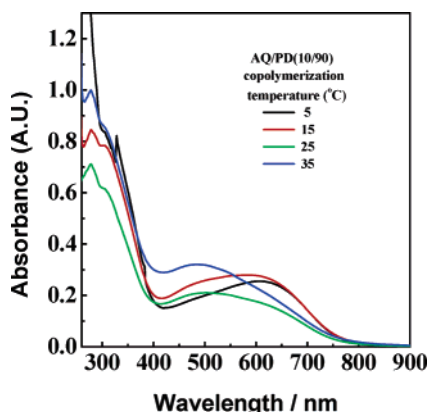


**Figure 8.** UV-vis spectra of the solution with a concentration of 0.0125 mg/mL in NMP of AQ/PD (10/90) copolymer bases prepared in 1 M HCl aqueous solution at 5–35 °C.

exhibits the highest intensity ratio of band II over I, possibly due to the relatively high polymerizability of AQ comonomer at a high temperature or in a neutral medium.

**3.4. <sup>1</sup>H NMR Spectra and Molecular Weight of the Copolymers.** It is found from 500 MHz <sup>1</sup>H NMR spectra of AQ/PD copolymer bases with seven AQ content from 0 to 100 mol % that the copolymers are typified by five main signals, corresponding to five kinds of protons. There is a strong distinct peak centered at 1.3 ppm and a relatively weaker peak at 4.1 ppm. Both of the peaks get steadily weaker as the PD content decreases, signifying that they are precisely due to –CH<sub>3</sub> and –OCH<sub>2</sub>– protons on the PD units, respectively. The weak peaks from 5.7 to 6.0 ppm could match up to the protons of primary amino groups at the ~NH<sub>2</sub> end group of polymer chain. The broad peaks in an extensive range from 6.3 to 9.7 ppm are ascribed to the aromatic protons on AQ and PD units. On the basis of an area comparison of the aromatic proton peak (6.3–9.7 ppm) on both AQ and PD units with –CH<sub>3</sub> proton peak (1.3 ppm) on only PD unit, it is feasible to evaluate the real AQ/PD molar ratio in the copolymers. The number of aromatic protons on AQ units may be anticipated through the following equation:

$$\text{AQ proton area} = \text{total aromatic proton area} - \text{methyl proton area} \quad (1)$$

Therefore

$$\text{molar ratio of AQ to PD} = (\text{AQ proton area}/5) / (\text{methyl proton area}/3) \quad (2)$$

The number-average degree of polymerization of AQ/PD copolymer could be approximately premeditated on the basis of the area comparison of the proton resonance peaks of –NH– over ~NH<sub>2</sub> groups by the following equation:

$$(\text{DP})_n = [2 \times (\text{–NH– proton area}) + (\text{~NH}_2 \text{ proton area})/2] / [(\text{~NH}_2 \text{ proton area})/2] \quad (3)$$

The results estimated thus are listed in Table 3. The actual AQ content of the copolymer appears higher than feed AQ content, suggesting that AQ monomer tends to homopolymerize rather than copolymerize with PD monomer. It is discovered that the AQ monomer is relatively favorable for the formation of the radical cation at the end of the growing chain to keep active as compared with PD monomer. The higher electron den-

**Table 3. Results Calculated from  $^1\text{H}$  NMR Spectra of 8-Aminoquinoline (AQ)/*o*-Phenetidine (PD) Copolymer Bases Prepared in 1 M HCl Aqueous Solution at 5 °C**

AQ/PD feed molar ratio	AQ/PD real molar ratio	degree of polymerization
0/100	0/100	16
10/90	11/89	20
30/70	37/63	23
50/50	65/35	14
100/0	100/0	13

**Table 4. Molecular Weight and Its Distribution of 8-Aminoquinoline (AQ)/*o*-Phenetidine (PD) Copolymer Bases Prepared in 1 M HCl Aqueous Solution at 5 °C**

AQ/PD feed molar ratio	$\overline{M}_n$ (g/mol)	$\overline{M}_w$	$\overline{M}_z$	$\overline{M}_w/\overline{M}_n$
0/100	1680	3210	5184	1.91
5/95	2000	5264	9701	2.64
10/90	1900	4337	7813	2.29

sity on the AQ quinoline ring makes the AQ radical cation more stable than PD radical cation and consequently gives it enough lifetimes to propagate. Moreover, the quinoline ring with higher electron density than PD ring is more likely to be attacked by the radical cation, leading to easier electrophilic aromatic substitution. Both of the factors finally result in a greatly augmented AQ content in the copolymer compared to AQ feed content and an increased degree of polymerization. Degree of polymerization increases first and then diminishes with increasing AQ content. AQ/PD (30/70) copolymer has the maximal degree of polymerization, possibly due to the two factors elaborated above, which coincides with the maximal band II intensity and the maximal intensity ratio of band III/I (Table 2). Besides, as the AQ content rises, greater steric hindrance of AQ ring might resist the formation of longer polymer chain.

It is found from Table 4 that the AQ/PD(10/90) copolymer base in THF also exhibits an increasing tendency of molecular weight with increasing AQ feed content from 0 to 10 mol %. Additionally, the GPC curves of AQ/PD copolymers exhibit a single peak with the polydispersity index from 1.91 to 2.64, which is similar to those of PAN and its derivatives.<sup>18</sup> Note that the molecular weight of the AQ/PD polymers determined by GPC is slightly lower than that by NMR because two measurements use THF and DMSO solvents.

### 3.5. Size of the Copolymer Particles in Water.

Usually, external stabilizer or dispersant is believed to be crucial to the synthesis of nanometer or even submicrometer particles by polymerization. Generally, the PAN particles with an average size of around 15  $\mu\text{m}$  were formed in situ by the oxidative polymerization without the external stabilizer.<sup>19</sup> If a sulfonic group as internal stabilizer was incorporated into the PAN side group, submicrometer particles of sulfonic aniline polymer with a mean diameter around 218 nm have been fabricated in situ by precipitation oxidative polymerization in our laboratory. In this study, submicrometer or even nanometer particles of AQ/PD copolymers without any sulfonic group or adding external stabilizer have been synthesized. Both the particle size and its distribution of AQ/PD copolymers analyzed by LPSA exhibit a significant dependency on the comonomer ratio, as shown in Figure 9. The number-average diameter ( $D_n$ ) of the virgin copolymer salts ranges from 5.611 to 9.135  $\mu\text{m}$ . After a dedoping treatment in  $\text{NH}_4\text{-OH}$ , both the  $D_n$  and its standard deviation of the base particles significantly decrease down to 315–4000 nm

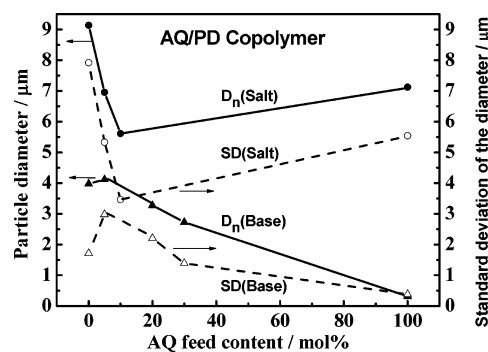


**Figure 9.** Particle diameter and its distribution of 8-aminoquinoline (AQ)/*o*-phenetidine (PD) copolymer particles (in water) with different AQ feed content obtained during in-situ copolymerization in 1 M HCl aqueous solution at 5 °C.

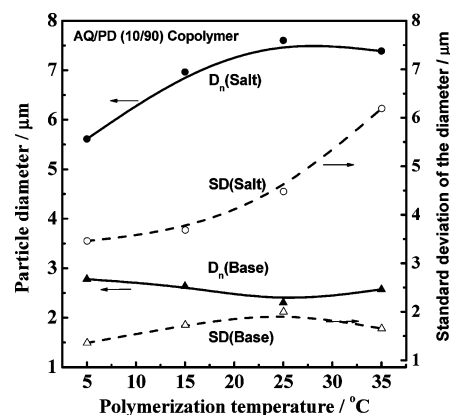
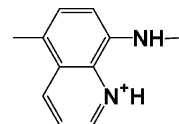


**Figure 10.** Particle diameter and its distribution of 8-aminoquinoline (AQ)/*o*-phenetidine (PD) (10/90) copolymer particles (in water) obtained during in-situ copolymerization in 1 M HCl aqueous solution at 5–35 °C.

### Scheme 2. Positively Charged Quaternary Ammonium Structures on the AQ Unit



and 380–3000 nm, respectively. Apparently, a transformation of the copolymer state from virgin salt to emeraldine base results in much smaller particle size, especially at a higher AQ content. This diminishing of the particle size could be ascribed to the exclusion of external dopants (HCl) on the copolymer chains, resulting in tight arrangement of copolymer chains and furthermore reduced size of the copolymer base particles. On the other hand, the lone electron pair on the AQ ring nitrogen is able to incorporate with  $-\text{N}^+\text{H}=\text{}$  in Scheme 2 to make copolymer chain display positive charge. Static rejection between the positive charges makes the chains less likely intertwine with each other and therefore keeps the copolymer particles less likely to gather. The higher the AQ content, the stronger the static rejection between copolymer chains is, leading to greatly reduced particle size. Note that the  $D_n$  of fine particles of AQ homopolymer base in water is only 315 nm, belonging to submicrometer order of magnitude.

Polymerization temperature has an influence on the particle size of the AQ/PD copolymer. As exhibited in Figure 10, the  $D_n$  of AQ/PD(10/90) copolymer particles exhibits an increasing tendency for virgin salt but nearly maintain a constant for emeraldine base with elevating

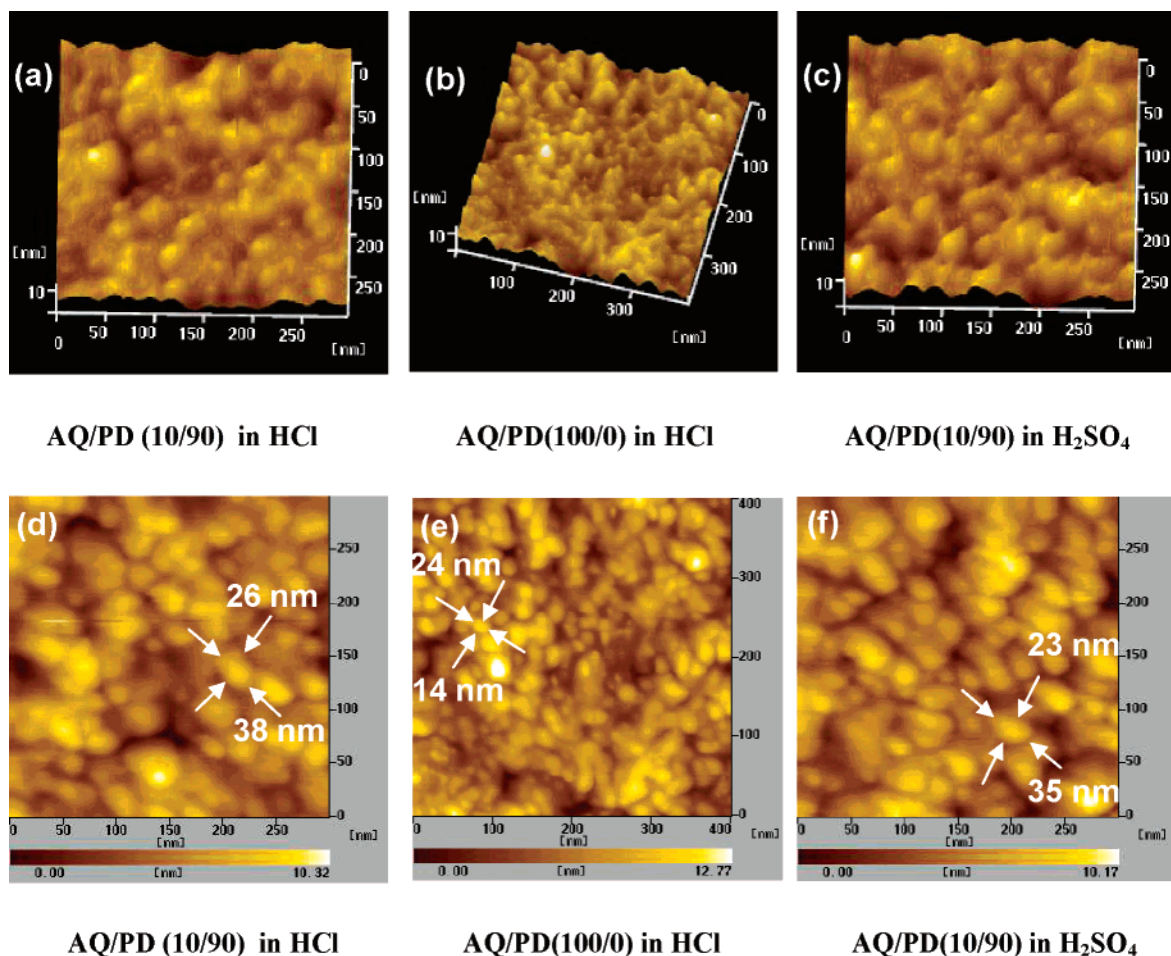


**Figure 11.** AFM three-dimensional images of (a) dry AQ/PD(10/90) copolymer particles formed in 1 M HCl at 5 °C, (b) dry AQ/PD(100/0) polymer base particles formed in 1 M HCl at 5 °C, (c) dry AQ/PD(10/90) copolymer base particles formed in 0.5 M H<sub>2</sub>SO<sub>4</sub> at 25 °C, and surface topography images of (d) dry AQ/PD (10/90) copolymer base particles formed in 1 M HCl, (e) dry AQ/PD-(100/0) polymer base particles formed in 1 M HCl, and (f) dry AQ/PD(10/90) copolymer base particles formed in 0.5 M H<sub>2</sub>SO<sub>4</sub> at 25 °C.

polymerization temperature from 5 to 35 °C. The increase of the salt particle sizes with elevating polymerization temperature may be primarily assigned to an increase in doping level resulted from increased quinoid content in the copolymer. Therefore, the dedoped bases formed at various temperatures exhibit similar particle size. However, the particle size of the dedoped bases of AQ/PD(10/90) copolymer exhibits a dependency on polymerization media, although polymerization medium has little effect on the particle size. As listed in Table 1, the copolymer base particles formed in 0.5 M H<sub>2</sub>SO<sub>4</sub> exhibit the smallest  $D_n$  of 441 nm, whereas the base particles formed in other two media are much larger. Therefore, the base particle size depends on the surrounding anions to some extent.

The size and shape of the copolymer base particles were further observed by AFM. The base particles look like ellipsoid shape, as shown in Figure 11. The ellipsoidal particles of AQ/PD (10/90) copolymer base formed in acidic polymerization medium have a major/minor axis diameters of 38/26 nm and 35/23 nm, respectively, while the ellipsoidal particles of AQ homopolymer have a smaller size with a major/minor axes of 24/14 nm. It is known that nanoparticles are generally prepared through an emulsion polymerization in which stabilizer, emulsifier, or dispersant is necessary, leading to complex composition of the product. In this paper, AQ/PD copolymer nanoparticles are facily

synthesized by precipitation chemical oxidative polymerization in the absence of any external additives. On the other hand, the nanoparticles obtained by the emulsion polymerization are usually spherical, while in this study ellipsoidal and pure nanoparticles are gained by the precipitation polymerization. It should be noticed that the particle size of the three polymers revealed by AFM is much smaller than that determined by LPSA. The smaller particle size observed by AFM than by LPSA should be recognized to contraction and compression of the particles because of the exclusion of water inside the particles during drying.<sup>20</sup> That is to say, microscopic AFM samples are equilibrium dry state in ambient air for AFM observation while LPSA samples are swollen in water. Another possible reason is that the AFM results are gained from a two-dimensional projection of image, but the LPSA outcomes are statistically treated by an equivalent sphere model.<sup>20</sup>

### 3.6. Electrical Conductivity of the Copolymers.

The oxidative polymers from aminoquinolines are expected to have an electrical conductivity like other heterocyclic aromatic amine polymers. The bulk electrical conductivity of AQ/PD copolymers obtained is shown in Figures 2 and 4 and Table 1. Obviously, the copolymer base particles with all AQ/PD ratios have a semi-conductivity of the magnitude from 10<sup>-11</sup> to 10<sup>-7</sup> S/cm and demonstrate minimal values in the AQ feed content between 5 and 50 mol %, which could be owing to the



**Table 5. Influence of 8-Aminoquinoline (AQ)/*o*-Phenetidine (PD) Feed Molar Ratio, Polymerization Temperature, and Polymerization Medium on the Solubility of 8-Aminoquinoline (AQ)/*o*-Phenetidine (PD) Copolymer Bases**

AQ/PD feed molar ratio	polymerization		solubility <sup>a</sup> and solution color <sup>b</sup>			
	temperature (°C)	medium	DMSO (7.2) <sup>c</sup>	NMP (6.7) <sup>c</sup>	CHCl <sub>3</sub> (4.1) <sup>c</sup>	THF (4.0) <sup>c</sup>
0/100	5	1 M HCl	PS, B	S, B	PS, P	S, B
5/95	5	1 M HCl	S, B	S, B	S, P	S, B
10/90	5	1 M HCl	S, B	S, B	S, BP	S, B
20/80	5	1 M HCl	S, RB	S, RB	S, RB	MS, RB
30/70	5	1 M HCl	S, RB	S, Br	SS	SS
50/50	5	1 M HCl	S, RB	PS, Br	SS	SS
100/0	5	1 M HCl	PS, RB	PS, RB	IS	IS
10/90	15	1 M HCl	S, BP	S, BP	S, BP	S, P
10/90	25	1 M HCl	S, PB	S, PB	S, PB	S, Br
10/90	35	1 M HCl	S, PB	S, PB	S, PB	S, PB
10/90	25	0.5 M H <sub>2</sub> SO <sub>4</sub>	S, PB	S, Br	S, PR	PS, PB
10/90	25	MeCN + H <sub>2</sub> O <sup>d</sup>	S, PB	S, Br	PS, Br	PS, Br

<sup>a</sup> IS = insoluble; MS = mainly soluble; PS = partially soluble; S = soluble; SS = slightly soluble. <sup>b</sup> B = blue; BP = bluish purple; Br = brown; P = purple; PB = purplish brown; PR = purplish red; RB = reddish brown. <sup>c</sup> The polarity index of the solvents. <sup>d</sup> Volume ratio of MeCN/H<sub>2</sub>O = 2/1.

copolymerization effect between AQ and PD comonomers. After doped in 1 M HCl aqueous solution for 48 h, their conductivity dramatically increases to  $10^{-7}$ – $10^{-5}$  S cm<sup>-1</sup>. Especially, the AQ/PD(5/95) copolymer exhibits the highest conductivity increase and also the highest conductivity in the six AQ/PD polymers upon redoping, possibly due to its highest molecular weight (also see Table 4). This behavior indicates that the conductivity of redoped AQ/PD copolymers is mainly related to their molecular weight.

It can be summarized from Figure 4 that the bulk electrical conductivity of HCl doped AQ/PD(10/90) copolymer rises with lowering polymerization temperature due to higher molecular weight of copolymer at lower temperature. However, the HCl-redoped AQ/PD(10/90) copolymers synthesized in three polymerization media exhibit similar conductivity. Note that the HCl-redoped AQ/PD copolymer prepared in 0.5 M H<sub>2</sub>SO<sub>4</sub> medium exhibits the highest conductivity of  $7.9 \times 10^{-7}$  S/cm. Therefore, the comonomer ratio, polymerization condition, and doping level can be all used to effectively control and adjust the conductivity of the AQ/PD copolymers.

**3.7. Solubility and Solvatochromism of the Copolymers.** Solubility of the AQ/PD copolymer base particles is investigated in four representative solvents with different polarity indexes. It is observed from Table 5 that the solubility can be significantly optimized by carefully controlling AQ/AS ratio and polymerization medium. With increasing AQ content, the AQ/PD copolymer exhibits a substantially decreased solubility in all the four solvents. When AQ/PD copolymers with the AQ feed content of not lower than 30 mol % are insoluble or slightly soluble in THF and CHCl<sub>3</sub>, despite of their relatively low molecular weight. This suggests that the lower solubility of the copolymer bases with higher AQ content may be largely ascribed to an enlarged chain rigidity or aromaticity of the polymers caused by more AQ units. Similar behavior has also been found in other nitrogen heterocyclic aromatic amine polymers.<sup>22</sup> Note that the AQ/PD copolymer bases containing AQ feed content of 5–50 mol % are completely soluble in NMP, but both PD and AQ homopolymers are only partly soluble in NMP as well as the AQ/PD copolymer bases containing AQ feed content of 5–20 mol % are completely soluble in CHCl<sub>3</sub>, but other AQ/PD polymers are partly soluble or even insoluble in CHCl<sub>3</sub>. That is to say, the AQ/PD copolymers obtained by the oxidative copolymerization are real copolymers containing both AQ

and PD units rather than a mixture of two homopolymers.

It is interesting that a color variation of AQ/PD copolymer solution with the solvents is observed, i.e., a novel solvatochromism. As listed in Table 5, the copolymer solution exhibits different colors within various solvents. The copolymer with AQ feed content less than 20 mol % is blue in NMP, DMSO, and THF and displays an inclination to violet in CHCl<sub>3</sub>. When AQ feed content is more than 20 mol %, the copolymer solution could be reddish-brown. The AQ/PD copolymer solution also exhibits different colors with changing polymerization temperature or medium or solvent, implying that their  $\pi$ -conjugated structure might change with polymerization condition or solvent used. In other words, the copolymer solvatochromism might be adjusted by choosing polymerization condition or solvent. It appears that most of the copolymer solutions are blue or violet of short wavelength, suggesting short conjugated length, i.e., low electrical conductivity, as discussed above. In addition, the copolymer solubility and solvatochromism depend on the solvent characteristics (for example, polarity index). Generally, NMP and DMSO with high polarity index are good solvents for the copolymers. However, there is no regular variation of the copolymer solvatochromism with solvent polarity index.

**3.8. Film Formability of the Copolymers.** The film formability is one of the most important processibilities for the new polymers.<sup>23</sup> However, few studies on the film formability of AQ polymers are reported so far. In this article, the film-forming ability of the polymer bases formed by the chemical oxidative polymerization has been studied. It is found that AQ/PD (5/95 and 10/90) copolymer bases prepared at polymerization temperature of 5 °C show good film formability. The films obtained exhibit strong adhesion to glass, shining bright luster because of very smooth surface without defects. Conversely, the film formability of the copolymer bases with higher AQ content is not good enough. It seems that superior solubility does not always mean better film formability. The good film formability of AQ/PD(10/90) copolymer bases might be ascribed to (1) higher molecular weight and (2) the formation of an actual solution, in which the copolymer chains could disperse homogeneously in the solvent rather than a system containing solid or swollen polymer fine particles scattered in the solvent emerging as a solution. Additionally, the redoped AQ/PD copolymer film exhibits slightly lower

electrical conductivity than corresponding pressed particle pellet because the relatively compact film could not be completely redoped by HCl.

#### 4. Conclusions

AQ/PD copolymerization was productively performed by a facile chemical oxidative precipitation polymerization for the synthesis of electrically semiconductive pure nanoparticles of the AQ/PD copolymers. The polymerization yield, molecular structure, particle diameter, bulk electroconductivity, solubility, solvatochromism, and film formability of the copolymers are fundamentally influenced by the comonomer ratio, polymerization temperature, and medium. That is to say, the polymerization feature, structure, and properties of the copolymers could be adjusted or even optimized by varying AQ/PD ratio and polymerization conditions. PD monomer is more easily oxidized to initiate the polymerization than AQ monomer, whereas AQ monomer with higher electron density on the quinoline ring could stabilize the activated end group and straightforwardly aid electrophilic aromatic substitution, leading to higher AQ content in the consequential copolymer chain than feed content. The AQ/PD copolymer demonstrates the maximal molecular weight, the maximal conductivity, and the best film formability at the AQ feed content of 5 mol % but exhibits minimal polymerization yield at the AQ feed content of 50 mol %. Low polymerization temperature or acidic medium is favorable for the synthesis of AQ/PD copolymers with high polymerization yield and long conjugated length. The particle size and its distribution of the copolymers exhibit a significant dependency on the comonomer ratio, alkaline treatment, polymerization temperature, and also medium. With increasing AQ content or elevating temperature, the mean diameter of the copolymer base particles reduces progressively. Shapes of nanoellipsoids with the major-/minor-axis diameter of 24 nm/14 nm and 38 nm/26 nm of the particles of AQ/PD(100/0) and (10/90) polymers prepared in 1 M HCl at 5 °C are discovered by AFM scrutiny. A facile technique of in-situ polymerization to synthesize pure nanoparticles of AQ/PD polymers without external stabilizer or internal sulfonic group is inaugurated. Positively charged qua-

ternary ammonium groups on the AQ units are critical for the formation and steady continuation of the nanoparticles.

**Acknowledgment.** The authors thank Prof. Dr. Roy G. Gordon in the Department of Chemistry and Chemical Biology of Harvard University for his valuable assistance. The project is supported by the National Natural Science Foundation of China (20174028).

#### References and Notes

- (1) Li, X. G.; Huang, M. R.; Duan, W.; Yang, Y. L. *Chem. Rev.* **2002**, *102*, 2925.
- (2) Belousova, L. I.; Vlasova, N. N.; Pozhidaev, Y. N.; Voronkov, M. G. *Russ. J. Gen. Chem.* **2001**, *71*, 1879.
- (3) Li, X. G.; Huang, M. R.; Li, S. X. *Acta Mater.* **2004**, *52*, 5363.
- (4) Huang, J.; Kaner, R. B. *J. Am. Chem. Soc.* **2004**, *126*, 851.
- (5) Zhang, X.; Manohar, S. K. *J. Am. Chem. Soc.* **2004**, *126*, 12714.
- (6) El-Rahman, H. A. A. *J. Appl. Electrochem.* **1997**, *27*, 1061.
- (7) Wen, T. C.; Chen, Y. H.; Gopalan, A. *Mater. Chem. Phys.* **2002**, *77*, 559.
- (8) An, H.; Seki, M.; Sato, K.; Kadoi, K.; Yosomiya, R. *Polymer* **1989**, *30*, 1076.
- (9) Ohno, N.; Wang, H. J.; Yan, H.; Tushima, N. *Polym. J.* **2001**, *33*, 165.
- (10) Choi, H. J.; Kim, J. W.; To, K. *Polymer* **1999**, *40*, 2163.
- (11) Gospodinova, N.; Terlemezyan, L. *Prog. Polym. Sci.* **1998**, *23*, 1443.
- (12) Wei, Y.; Hsueh, K. F.; Jang, G. W. *Polymer* **1994**, *35*, 3572.
- (13) Li, X. G.; Chen, R. F.; Huang, M. R.; Zhu, M. F.; Chen, Q. *J. Polym. Sci., Part A: Polym. Chem.* **2004**, *42*, 2073.
- (14) Han, C. C.; Hong, S. P.; Yang, K. F.; Bai, M. Y.; Lu, C. H.; Huang, C. S. *Macromolecules* **2001**, *34*, 587.
- (15) Naoi, K.; Suematsu, S.; Manago, A. *J. Electrochem. Soc.* **2000**, *147*, 420.
- (16) Azzem, M. A.; Yousef, U. S.; Limosin, D.; Pierre, G. *J. Electroanal. Chem.* **1996**, *417*, 163.
- (17) Wei, Y.; Hsueh, K. F.; Jang, G. W. *Macromolecules* **1994**, *27*, 518.
- (18) Mattoso, L. H. C.; Manohar, S. K.; MacDiamid, A. G.; Epstein, A. J. *J. Polym. Sci., Part A: Polym. Chem.* **1995**, *33*, 1227.
- (19) Min, G. *Synth. Met.* **2001**, *119*, 273.
- (20) Li, X. G.; Zhou, H. J.; Huang, M. R.; Zhu, M. F.; Chen, Y. M. *J. Polym. Sci., Part A: Polym. Chem.* **2004**, *42*, 3380.
- (21) Pullen, A. E.; Swager, T. M. *Macromolecules* **2001**, *34*, 812.
- (22) Huang, M. R.; Li, X. G.; Yang, Y. L. *Polym. Degrad. Stab.* **2001**, *71*, 31.
- (23) Li, X. G.; Huang, M. R.; Zhu, M. F.; Chen, Y. M. *Polymer* **2004**, *45*, 385.

MA047581N